ELSEVIER

Ceramics International 27 (2001) 91–97

CERAMICS INTERNATIONAL

www.elsevier.com/locate/ceramint

Study of the solid state reaction and the morphotropic phase boundary in $Pb(Zr, Ti)O_3$–$Pb(Fe_{1/5}, Ni_{1/5}, Sb_{3/5})O_3$ ceramics

Ahmed Boutarfaia *

Institut des Sciences Exactes, Université Mohamed Khider-Biskra, BP 145, RP-Biskra (07000), Algeria

Received 15 November 1999; received in revised form 3 January 2000; accepted 1 March 2000

Abstract

The formation mechanisms of $Pb(Zr_{0.46}, TiO_{0.49})O_3$–$0.05Pb(Fe_{1/5}, Ni_{1/5}, Sb_{3/5})O_3$ ternary solid solution prepared by the mixed oxides techniques has been characterized by X-ray diffraction (XRD), differential thermal analysis (DTA) and thermal gravimetric analysis (TGA). In a previous investigation (part I), we have shown that the formation of PZT is accomplished through several steps: decomposition of Pb_3O_4 to PbO; formation of $PbTiO_3$ above 350°C and of its solid solutions at 650°C. This second part of the work aims to study the morphotropic phase boundary (MPB). Piezoelectric ceramics having a composition of $x\ PbZrO_3$–$(0.95\text{-}x)PbTiO_3$–$0.05\ Pb(Fe_{1/5}, Ni_{1/5}, Sb_{3/5})O_3$ and a Zr/Ti ratio between 44/51 and 52/43 were prepared in the 850–1200°C temperature range. The morphotropic phase boundary (MPB) of the solid solution is located at $x = 47$–50.

Keywords: A. Calcination; B. X-ray methods; C. Piezoelectric properties; D. PZT

1. Introduction

$Pb(Zr_x, Ti_{1-x})O_3$ (PZT) perovskites have been extensively studied with the aim to optimize their piezoelectric properties [1]. PZT has been a standard piezoelectric material for the past forty years. The Zr/Ti ratio is known to strongly influence properties, such as the elastic constant, the piezoelectric constant, the permittivity, the coupling factor, etc. Near the morphotropic phase boundary (MPB), all these properties take extreme values when x corresponds to the composition of the morphotropic phase boundary (MPB) which separates the tetragonal (T) and rhombohedral (R) phases towards Ti-rich and Zr-rich sides, respectively.

1.1. Formation of PZT

The formation of $Pb(Zr_x, Ti_{1-x})O_3$ has been studied with several kinds of starting materials by several authors who suggested a large number of reaction mechanisms [2–12]. The phase assemblages and appearance of intermediate reaction products will depend on the precursor powders that have been employed (specifically, their purity and particle size) and the time and temperature at which the solid state reaction has been allowed to proceed. To investigate the reaction sequence through which PZT solid solutions are formed by solid-state reactions in a mixture of $PbO + TiO_2 + ZrO_2$, researchers have performed several series of calcination tests, but came up with different conclusions. There have been contradictory observations, particularly with respect to the presence or absence of intermediate products like $PbZrO_3$, a $PbTiO_3$ solid solution (PT)ss and a PbO solid solution (P)ss.

1.2. Co-existence of phases

The precise determination of the MPB composition range, which is believed to be quite narrow, has attracted immense interest [13]. Thermodynamically, the MPB is expected to be a two-phase region over which the rhombohedral and tetragonal phases coexist [14,15]. Most studies have shown that the morphotropic phase change takes place at a specific ratio of Zr to Ti in the PZT solid solution [16–20], whereas another of investigators has demonstrated that there can be co-existence of tetragonal-rhombohedral phases over a wide range of

* Tel.: +213-4-74-7789; fax: +213-4-74-0730.

0272-8842/01/$20.00
PII: S0272-8842(00)00047-X

compositions around the morphotropic phase boundary (MPB) [15,21–25]. Investigations of the $Pb(Zr_x, Ti_{1-x})O_3$ system have shown the existence of an almost temperature independent morphotropic phase boundary at $x = 0.52$–0.53, which separates a rhombohedral phase from a tetragonal one. By means of X-ray diffraction, the co-existence of the two phases over a range of compositions around the MPB was demonstrated. Many authors have shown that the co-existence of the two phases at the MPB is due to the frozen-in compositional fluctuations at the Zr/Ti site because of the diffusional limitations of the conventional solid state processing route.

The aim of the present work is (i) to study the mechanism of PZT solid solution formation and to determine the temperature of formation of PZT; (ii) to determine the width of the two phase region and the exact composition of the MPB in the $x\,PbZrO_3$–$(0.95-x)$ $PbTiO_3$–0.05 $Pb(Fe_{1/5}, Ni_{1/5}, Sb_{3/5})O_3$ system by X-ray diffractometry (XRD) in conjunction with the evaluation of electromechanical properties, was used.

2. Experimental details

Ceramics of composition $xPbZrO_3$–$(0.95–x)PbTiO_3$–$0.05Pb(Fe_{1/5}, Ni_{1/5}, Sb_{3/5})O_3$ near the rhombohedral–tetragonal morphotropic phase boundary, were prepared from mixed oxides. The mixtures were made from crystalline raw materials of high purity: Pb_3O_4 (99.9%), TiO_2 (99.56%), ZrO_2 (99.9%). The following oxides were used as additives: NiO (99.9%), Fe_2O_3 (99.9%) and Sb_2O_3 (99.9%). The characteristics of the powders are given in Table 1.

2.1. Sample preparation for reaction mechanism of PZT

For this study, a single composition, $Pb(Zr_{0.46}, TiO_{0.49})O_3$–0.05 $Pb(Fe_{1/5}, Ni_{1/5}, Sb_{3/5})O_3$ was chosen. The corresponding molar fractions were weighted and wet mixed in stoichiometric ratios in a ball mill. 50 g of each composition was weighed and wet mixed for 6 h in acetone. Each batch was dried at 120°C for 3–4 h, remixed, and divided in 10 parts. The mixtures were dried and pressed with into pellets at 1000 kg/cm^2, and then allowed to react at the desired temperature for 2 h in a small corundum crucible. The heating rate were 1 to 6°C/min, and the temperatures were 300, 350, 400, 450, 500, 600, 650, 700, 750 and 800°C. Then the samples were air quenched to room temperature and ground in an agate mortar. Powder X-ray diffraction tests were carried out using a D500 Siemens with CuK_α radiation and nickel filter. DTA/TGA was conducted with Al_2O_3 as the reference material. Data curves for this 0.46 $PbZrO_3$–0.49 $PbTiO_3$–0.05 $Pb(Fe_{1/5}, Ni_{1/5}, Sb_{3/5})O_3$ composition were obtained from 25 to 1000°C. The amount of uncombined PbO in the fired samples was determined by chemical analysis. A weighed sample was treated with 6 N acetic acid, in which only uncombined PbO was soluble, and the amount of PbO was determined by EDTA titration using xylenol orange as an indicator.

Table 1
Characteristics values of raw materials

Material	Purity (%)	Phase	Particle size (μm)
Pb_3O_4	99.0	Orthorhombic	3.2
TiO_2	99.56	Tetragonal	0.6
ZrO_2	99.9	Monoclinic	0.8

2.2. Sample preparation for determination of co-existence of phases

2.2.1. Crystallographic structure

In order to investigate the morphotropic phase boundary samples were prepared according to the formula: $xPbZrO_3$–$(0.95-x)$ $PbTiO_3$–0.05 $Pb(Fe_{1/5}, Ni_{1/5}, Sb_{3/5})O_3$, where $44 < x < 52$. The crystallography of the phases present in the compositions was determined using XRD analysis of finished ceramics, sintered from 850 to 1180°C in a PbO atmosphere for 2 h. The tetragonal, rhombohedral and tetragonal–rhombohedral phases were identified by an analysis of the peaks [002 (tetragonal), 200 (rhombohedral), 200 (tetragonal)] in the 2θ range 43–46° and their lattice parameters were calculated. In order to ensure an accurate determination of the lattice parameters, the X-ray peaks were recorded gradually in steps of 0.01°.

2.2.2. Electrical measurements

For measurement of piezoelectric properties, the samples were prepared by the usual ceramic technique. The oxides were mixed mechanically during 10 h in batches of about 80 g and pressed at 1200 kg/cm^2 into pellets of about 15–20 mm high and 13 mm diameter. After mixing, pre-firing of the powders took place at 800°C for 2 h, followed by dry ball-milling for 30 h. The calcined powders were ground thoroughly, and specimen discs were made with a diameter of 12 mm and a thickness of 0.8 mm, were pressed at 14 000 kg/cm^2. These specimens were sintered in almost closed corundum crucibles in controlled PbO atmosphere at 1150°C. It was verified after each sintering run that there was no weight loss in the pellets due to the possible escape of PbO at high temperatures. After sintering, the silver paste was fired onto the faces of ceramics at 750°C for 30 min. The samples were poled in silicon oil at 110°C by applying a static field of 35 kV/cm for 60 min. The dielectric constant of the samples was also measured before and after poling, at 10 kHz. Properties such as kp, S_{11} and d_{31} were measured by a method similar to that of the IRE standard resonance method.

The resonance and antiresonance frequencies were obtained using the maximum and minimum of admittance spectra.

3. Results and discussion

3.1. Formation of $Pb(Zr_{46}, Ti_{49})O_3$–5 $Pb(Fe_{1/5}, Ni_{1/5}, Sb_{3/5})O_3$

The X-ray powder diffraction analysis showed that the Pb_3O_4 disappeared partially and that lead oxide (PbO) appeared over a narrow temperature range 350–650°C. Fig. 1 shows the DTA/TGA curves obtained from the mixed oxide sample over the temperature range 190–560°C. The endothermic peak observed at about 240°C is due to Pb_3O_4 decomposition. An appreciable weight loss of 2.5% is found with TGA. The DTA curve shows an endothermic signal at 560°C, which is related to Pb_3O_4 final decomposition. The first reaction taking place is:

$$Pb_3O_4 \rightarrow 3\ PbO + 1/2O_2 \quad (1)$$

$PbTiO_3$ formation starts at 350°C and is exothermic in nature. The products contain PbO, TiO_2 and traces of Pb TiO_3, which indicates that below 350°C the reaction proceeds only at intergranular PbO–TiO_2 boundaries according to the following equation:

$$PbO + TiO_2 \rightarrow PbTiO_3 \quad (2)$$

The results of differential scanning calibration (DSC) analysis confirmed the start of an exothermic reaction at 350°C. This reaction is believed to represent lead titanate formation as the formation enthalpy of $PbTiO_3$ is lower than that of $PbZrO_3$. The formation of lead titanate at lower temperature (350°C) can be explained by the high activity of TiO_2 and of lead oxide (PbO) produced from Eq. (1). XRD analysis of quenched samples indicated that formation of $PbTiO_3$ was complete at 650°C as shown by the disappearance of the lines corresponding to TiO_2. The parameters of the tetragonal lattice of lead titanate at 500, 600 and 650°C were calculated from d_{200} and d_{002} corresponding to a_T and c_T, respectively. The results are presented in Fig. 2. A small variation in the c_T/a_T ratio is observed and it is proposed that over the narrow temperature range, the reaction proceeds at $PbTiO_3$–PbO and $PbTiO_3$–ZrO_2 boundaries, and that PbO and ZrO_2 diffuse into the lead titanate perovskite lattice to form a solid solution. Furthermore, the intensity of the diffraction lines for lead titanate do not change, and those corresponding to the PbO and ZrO_2 slightly decrease. Therefore, the third reaction step is:

$$PbTiO_3 + xPbO + xZrO_2 \rightarrow Pb_{1+x}TiZr_xO_{3+3x} \quad (3)$$

The saturated lead titanate solid solution acts as a basis for the PZT formation. It seems that diffusion of Pb^{+2} and Zr^{+4} ions in the lead titanate perovskite surface results in the formation of PZT. A final thermal effect at approximately 650°C was also found. In this case the endothermic peak can be attributed to PZT formation which is an endothermic process. In Fig. 3, XRD analysis for the saturated reactants calcined at 650, 700, 750 and 800°C is shown to result in PZT formation. The reaction in this final step is stated below:

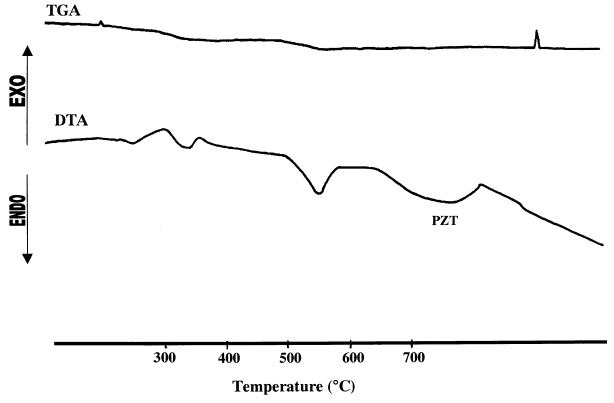

Fig. 1. DTA/TGA curves for: 46$PbZrO_3$–49$PbTiO_3$–5Pb($Fe_{1/5}$, $Ni_{1/5}$, $Sb_{3/5}$)O_3 composition.

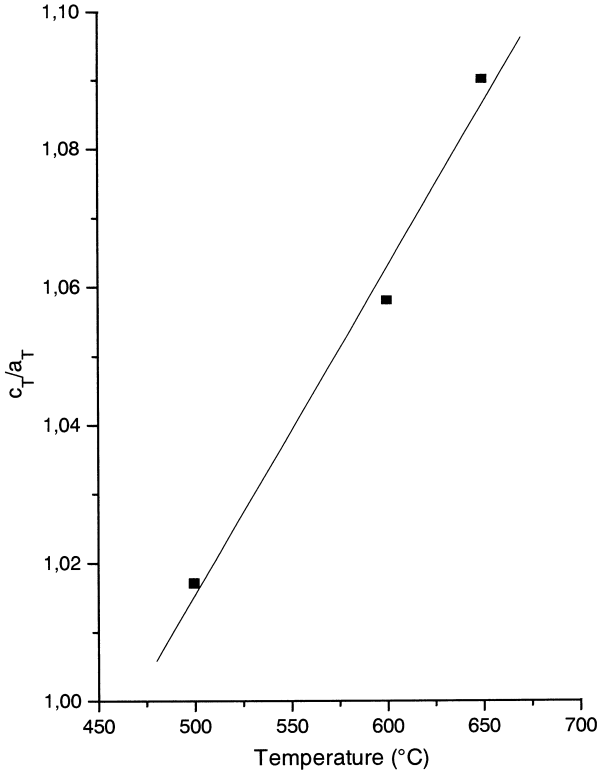

Fig. 2. Variations ratio c_T/a_T of $PbTiO_3$ of calcing at temperature indicated.

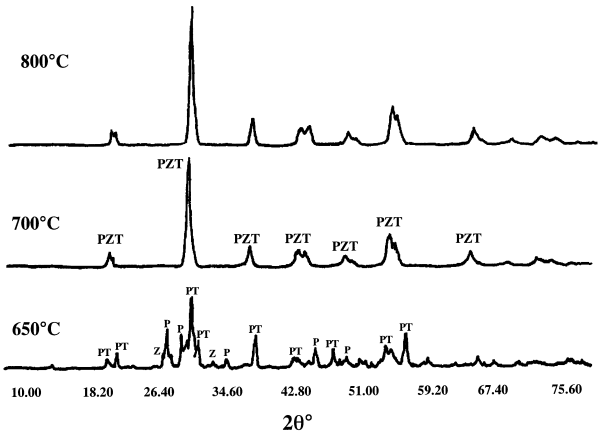

Fig. 3. X-ray diffraction patterns of standard reactants calcined at 650, 700 and 800°C.

$$PbTiO_3 + PbO + ZrO_2 \rightarrow (PZT)ss \quad (4)$$

It is important to note the absence of $PbZrO_3$. At 700°C, a total disappearance of the solid solution of lead titanate and of reactant oxides was observed. However, the chemical analysis of samples calcined at 650, 700 and 800°C indicated that a small amount of free PbO was present. This is probably due to an excess of PbO in the initial mixture. The formation of PZT solid state at lower temperature was explained by the presence of the dopants Fe_2O_3, NiO and Sb_2O_3.

3.2. Optimization of sintering temperature

Fig. 4 shows the density for 47 $PbZrO_3$–48 $PbTiO_3$–5 $Pb(Fe_{1/5}, Ni_{1/5}, Sb_{3/5})O_3$ samples as a function of sintering temperature. The density increases with sintering temperature in the initial period and saturates beyond 1150°C. The density of the sintered samples was calculated from the sample dimensions and weights. The firing temperature leading to the maximum density, ρ, lies between 1050 and 1180°C. At 1150°C, 97% of the theoretical value was achieved. As shown in Fig. 4, the sintered density of the PZT–PFNS specimen decreases slightly as sintering temperature increases (above 1150°C). The optimum sintering temperature was defined as the point when the PbO vapor pressure evaporation-recondensation equilibrium was reached. The optimum value of the sintering temperature is affected by the addition of impurities and other processing parameters such as the rate of heating, duration of thermal treatment, and protecting. In view of this observation, we decided to sinter the PZT–PFNSb pellets at 1150°C.

3.3. Location of the morphotropic phase boundary

3.3.1. X-ray powder diffraction studies

Sintered powders were examined by X-ray diffractometry to ensure phase purity and to identify the

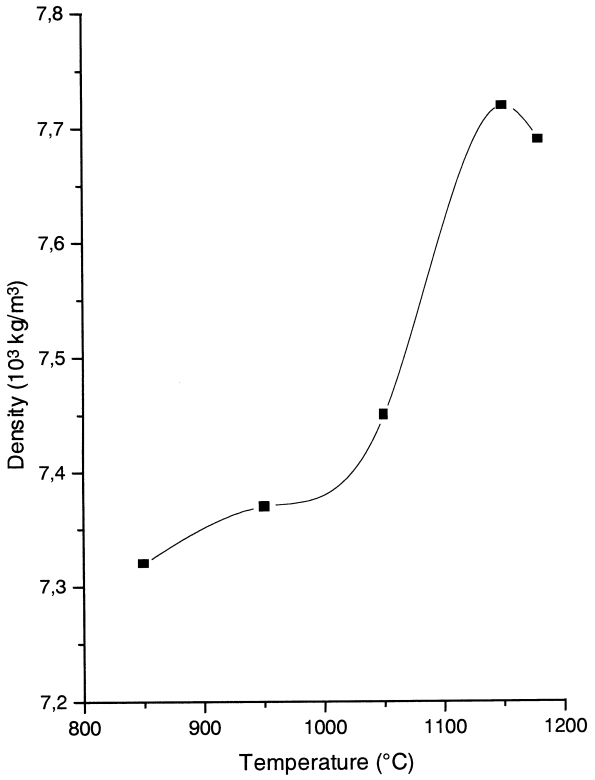

Fig. 4. Density versus sintering temperature for PZT–PFNS ceramics (sintering time 2 h).

phases and lattice constants of the materials. The co-existence of tetragonal and rhombohedral phases near the morphotropic phase boundary implies the existence of compositional fluctuations. The compositional fluctuation can in principle be determined from the width of the X-ray diffraction peaks. However, determination of the compositional fluctuation for samples near the morphotropic phase boundary is difficult. XRD patterns of PZT powders were analyzed to detect the characteristic rhombohedral and tetragonal splitting. A morphotropic phase boundary "co-existence region" was observed [shown by duplicated (200) peaks]. It has been reported in the literature that the splitting of these reflections into triplets takes place in conventionally-prepared ceramics due to compositional fluctuations leading to the co-existence of the tetragonal and rhombohedral phases [15].

The results of XRD (at room temperature) of the peak (200) in the $x PbZrO_3$–$(0.95-x)PbTiO_3$–0.05Pb $(Fe_{1/5}, Ni_{1/5}, Sb_{3/5})O_3$ for several compositions are shown in Fig. 5. Triplet peaks around $2\theta = 45°$ indicate that the specimen consists of a mixture of tetragonal and rhombohedral phases. A transition from rhombohedral to tetragonal phase is observed as the concentration of $PbTiO_3$ increases. The transition zone is a region where both phases exist simultaneously. It is shown that the tetragonal structure can be formed up to $x_T < 47$ while the rhombohedral structure stabilize at $x_R > 50$. At $x = 47-50$, the tetragonal and rhombohedral phases

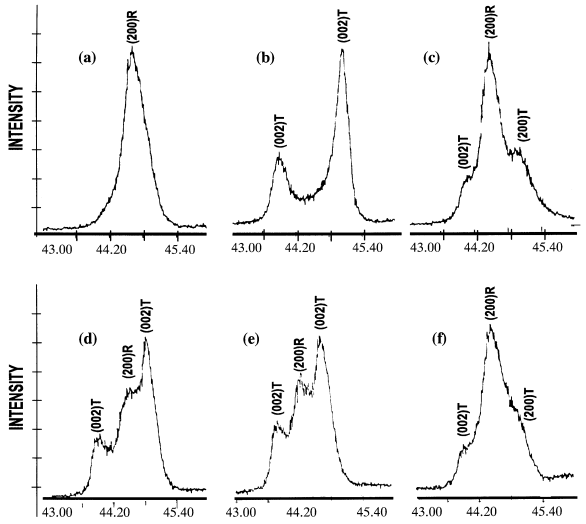

Fig. 5. X-ray diffraction patterns of xPbZrO$_3$–y PbTiO$_3$–5 Pb(Fe$_{1/5}$, Ni$_{1/5}$, Sb$_{3/5}$)O$_3$ after crushing the pellets at 1150°C for 2 h: (a) x/y, 51/44; (b) x/y 46/49; (c) x/y, 50/45; (d) x/y, 49/46; (e) x/y, 48/47; (f) x/y, 47/48. The co-existence of tetragonal and rhombohedral splitting in the (c, d, e, f).

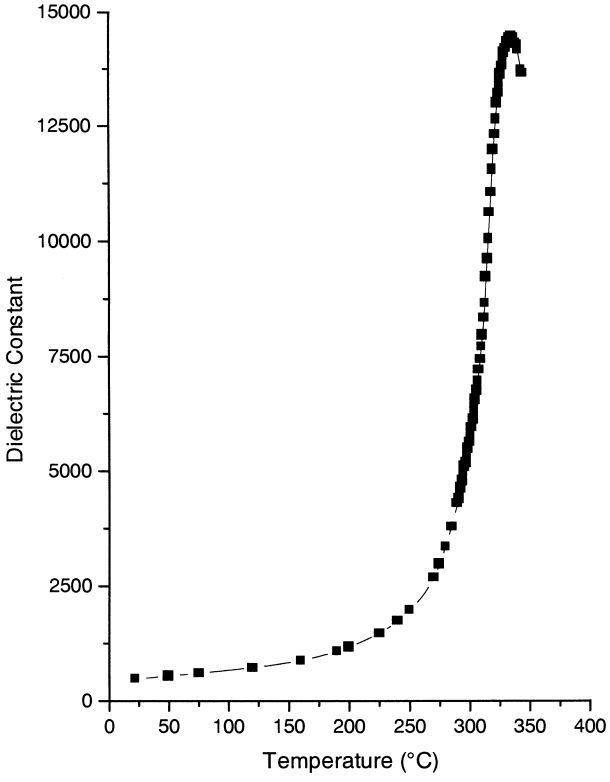

Fig. 6. Dielectric constant (ε) at room temperature as a function of temperature.

coexist. The co-existence region is therefore quite narrow ($\Delta x = 0.03$) and extends between x_T and x_R. The region in which two phases co-exist is stable throughout the interval from x_T and x_R, although one of these phases may be metastable relative to the other phase in one part of this interval and vice versa in the other part. The width $\Delta x = x_T - x_R$ of the co-existence region obtained from our work is close to that reported by many authors. This can be explained by microscopic compositional fluctuations occurring in these perovskite materials, which cannot provide a real homogeneity in the solid solutions, and also by the different stresses induced in the ceramic grains, which determined the co-existence of tetragonal-rhombohedral phases. An increase in sintering temperature and firing time enhanced the diffusion effects within these regions and led to a relative homogenization of the local composition of the material.

3.3.2. Dielectric and piezoelectric studies

The dielectric constant (ε), the electromechanical coupling factor (kp), the piezoelectric constant (d_{31}) and Young's modulus (S_{11}) were measured for specimens of various compositions sintered at 1150°C.

Fig. 6 shows the temperature dependence of ε of 0.47 PbZrO$_3$–0.48 PbTiO$_3$–0.05 Pb(Fe$_{1/5}$, Ni$_{1/5}$, Sb$_{3/5}$), as a typical example of a PZT–PFNSb ceramic. The dielectric constant, which is equal to 297 at room temperature, increased to a peak value of 14 473 at the transition temperature $T_c = 335$°C (PbZrO$_3$ has a transition temperature of 230°C). The temperature of the maximum dielectric constant corresponds to the ferroelectric Curie temperature.

Fig. 7 shows the values of the piezoelectric charge constant d_{31} as a function of composition for xPbZrO$_3$–$(0.95-x)$ PbTiO$_3$–0.05 Pb(Fe$_{1/5}$, Ni$_{1/5}$, Sb$_{3/5}$) for x in the range of 0.44–0.52. In this figure, the value of increases as the concentration of PbZrO$_3$ increases and shows a maximum value for the composition 0.47 PbZrO$_3$–0.48 PbTiO$_3$–5 Pb(Fe$_{1/5}$, Ni$_{1/5}$, Sb$_{3/5}$).

The evaluation results of the planar coupling coefficients kp are shown in Fig. 8. PZT–PFNS exhibits very large kp values around the MPB. At this composition, the value of kp equals 0.63. Thus from the trend of the variation of electromechanical properties and their optimum values, it is would appear that the MPB lies at approximately 47/48 = Zr/Ti ratio in PZT solid solution. At the transition region, piezoelectricity reaches its maximum value due to the piezoelectric interactions among the existing five domains, two of which belong to the tetragonal phase (180° and 90°) and three to the orthorhombic phase (180°, 71°, and 109°).

Young' modulus for the system PZT–PFNSb is shown in Fig. 9 for different compositions with an increasing Zr/Ti ratio. The value of Y decreases as the PbZrO$_3$ concentration increases, and Y attains a minimum value at Zr/Ti = 47/48. It can be seen that all curves are characterized by an initial gradual decrease in the values of Young's modulus, reaching a minimum value near the transition. This can be explained by the gradual decrease

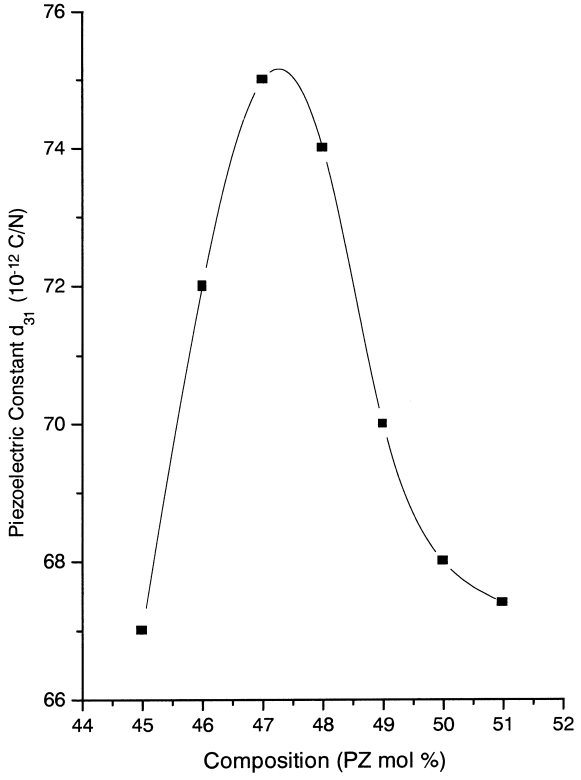

Fig. 7. d_{31} at room temperature as a function of mol% PZ for PZT–PFNSb.

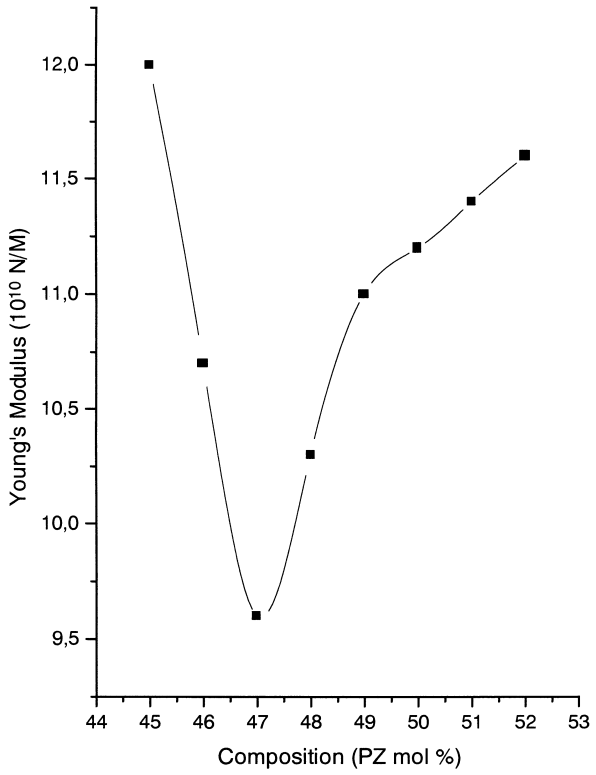

Fig. 9. Variation of S_{11} with composition (mol% PZ) for PZT–PFNSb.

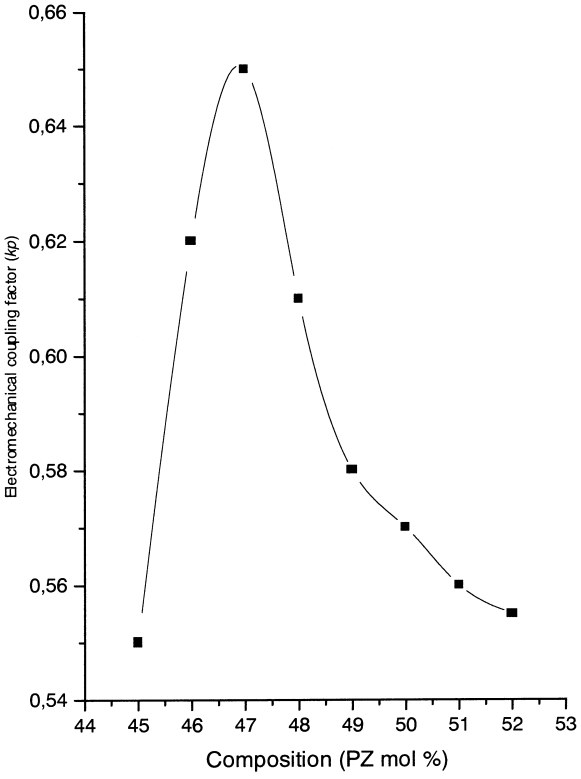

Fig. 8. Variation of *kp* with composition (mol% PZ) for PZT–PFNSb.

of tetragonality and the pronounced drop of the curves near the phase transition Zr/Ti = 47/48. The optimal electromechanical properties are obtained with the composition 0.47$PbZrO_3$–0.48 $PbTiO_3$–0.05$Pb(Fe_{1/5}, Ni_{1/5}, Sb_{3/5})$.

4. Conclusions

1. The formation mechanism of PZT solid solution with a small amount of Fe_2O_3, Sb_2O_3 and NiO was studied by the mixed oxides consisting of Pb_3O_4, TiO_2 and ZrO_2. The first step is the decomposition of Pb_3O_4 on PbO. The second step, above 350°C, is the reaction of PbO and TiO_2 to form $PbTiO_3$. When the saturated $PbTiO_3$ is submitted to a temperature increase, the interaction of PbO, ZrO_2 and TiO_2 inside the $PbTiO_3$ perovskite forming the PZT solid solution takes places. The differences found with respect to the reaction mechanism reported by other authors may be due to different experimental conditions.
2. The phase and microstructure of the sintered samples were examined by X-ray diffractometry (XRD). In this work, the solid solution $x$$PbZrO_3$–(0.95−$x$) $PbTiO_3$–0.05$Pb(Fe_{1/5}, Ni_{1/5}, Sb_{3/5})O_3$ were studied. The morphotropic phase boundary (MPB) of the

solid solution is located at $x = 47$–50 and there is a coexistence of tetragonal and rhombohedral phases even in compositionally homogeneous PZT powders. The electromechanical coupling factor (kp) and the dielectric constant reach their maximum at the new MPB.

References

[1] B. Jaffe, R. Cook, H. Jaffe, Academic Press, London/New York, 1971.
[2] T. Ohno, M. Takahashi, N. Tsubouchi, J. Jap. Soc. Powder Metall. 20 (1973) 154.
[3] Y. Matsuo, H. Sasaki, J. Am. Ceram. Soc. 48 (1965) 289.
[4] D.L. Hankey, J.V. Biggers, J. Am. Ceram. Soc. 64 (1981) 172.
[5] S.S. Chandratreya, R.M. Fularth, J.S. Pask, J. Am. Ceram. Soc. 64 (1981) 422.
[6] S. Venkataramany, J.V. Biggers, Ceram. Soc. Bull. 59 (1980) 462.
[7] A.I. Kingon, P.J. Terblanche, J.B. Clark, Ceram. Int. 8 (1982) 108.
[8] B.V. Hirmeth, A.I. Kingon, J.V. Biggers, J. Am. Ceram. Soc. 66 (1983) 790.
[9] E. Jaran, P. Duran, J. Physique, Coll. 47 (Suppl. 2) (1986) 537.
[10] V.M. Speri, PhD thesis, Rutgers University, NJ, 1969.
[11] S. Mori, H. Mitsuda, K. Date, Y. Kioki, T. Miyazida, Nat. Tech. Dept. 10 (1964) 32.
[12] T. Yamaguchi, S.H. Sho, M. Maomori, H. Kuno, Ceramurgia Int. 2 (1976) 76.
[13] T. Kakegawa, J. Mohri, K. Takahashi, H. Yamamura, S. Shirasaki, Solid State Commun. 24 (1977) 769.
[14] P. Ari-Gur, L. Benguigui, Solid State Commun. 15 (1974) 1077.
[15] V.A. Isupov, Solid State Commun. 17 (1975) 1331.
[16] E. Sawaguchi, J. Phys. Soc. Japan 8 (1953) 615.
[17] B. Jaffe, R. Cook, S. Marzullo, J. Res. Natl. Bur. Stand. 55 (1955) 239.
[18] D.A. Berlincourt, C. Cmolik, H. Jaffe, Proc. I.R.E. 48 (1960) 220.
[19] K. Karl, K.H. Hardtl, Phys. Stat. Sol. 8 (1971) 87.
[20] A. Pinczuk, Solid State Commun. 12 (1973) 1035.
[21] P. Ari-Gur, L. Benguigui, J. Phys. D 8 (1975) 1856.
[22] L. Benguigui, Solid State Commun. 19 (1976) 979.
[23] L.D. Landav, E.M. Lifshitz, Statistical Physics, Pergamon Press, London, 1959.
[24] A. Boutarfaia, C. Boudaren, A. Mousser, S.E. Bouaoud, Ceram. Int. 21 (1995) 391.
[25] A. Boutarfaia, S.E. Bouaoud, Ceram. Int. 22 (1996) 282.